

THE SEMILEPTONIC B TO $K_1(1270, 1400)$ DECAYS IN QCD SUM RULES

H. Dağ^{1,2,*}, A. Özpineci^{1,†}, M. T. Zeyrek^{1,‡}

¹ *Department of Physics, Middle East Technical University,
06531 Ankara, Turkey.*

² *Laboratory for Fundamental Research , Özyeğin University,
Kusbakisi Cad. No:2, Altunizade-Uskudar,
34662, Istanbul, Turkey.*

*e-mails: *huseyin.dag@cern.ch,*

†ozpineci@metu.edu.tr, ‡zeyrek@metu.edu.tr

We analyze the semileptonic rare decays of B meson to $K_1(1270)$ and $K_1(1400)$ axial vector mesons. The $B \rightarrow K_1(1270, 1400)\ell^+\ell^-$ decays are significant flavor changing neutral current decays of the B meson. These decays are sensitive to the new physics beyond SM, since these processes are forbidden at tree level at SM. These decays occurring at the quark level via $b \rightarrow s\ell^+\ell^-$ transition, also provide new opportunities for calculating the CKM matrix elements V_{bt} and V_{ts} . In this study, the transition form factors of the $B \rightarrow K_1(1270, 1400)\ell^+\ell^-$ decays are calculated using three-point QCD sum rules approach. The resulting form factors are used to estimate the branching fractions of these decays.

PACS numbers: 11.55.Hx, 12.38.Lg, 13.20.Eb

I. INTRODUCTION

In standard model (SM), the flavor changing neutral current (FCNC) decays of B meson are forbidden at tree level and occur only at loop level. These decays are good candidates for searching new physics (NP) beyond SM or the modifications on the SM. Some of these rare FCNC decays of B meson; semileptonic and radiative decays into a vector or an axial vector meson, such as $B \rightarrow K^*(892)\gamma$ [1–3], $B \rightarrow K_1(1270, 1400)\gamma$ [4] and $B \rightarrow K^{0*}(892)e^+e^-(\mu^+\mu^-)$ [5, 6] have been observed. For the channel $B \rightarrow K^*(892)\ell^+\ell^-$, the measurement of isospin and forward backward asymmetries at BaBar are also reported[7–9]. For the radiative decays of B meson into $K_1(1270, 1400)$ axial vector meson states, Belle reported the following branching fractions[10]:

$$\begin{aligned} \mathcal{B}(B^+ \rightarrow K_1(1270)^+\gamma) &= (4.28 \pm 0.94 \pm 0.43) \times 10^{-5}, \\ \mathcal{B}(B^+ \rightarrow K_1(1400)^+\gamma) &< 1.44 \times 10^{-5}. \end{aligned} \quad (1)$$

The semileptonic $B \rightarrow K_1(1270, 1400)\ell^+\ell^-$ decays are significant FCNC decays of B meson, which occur via $b \rightarrow s\ell^+\ell^-$ transitions at quark level. The semileptonic decay modes $B \rightarrow K_1(1270, 1400)\ell^+\ell^-$ have not been observed yet, but are expected to be observed in forthcoming pp and e^+e^- accelerators, such as LHC[12] and SuperB[13]. In particular LHCb experiment at the LHC could be the first place to observe such decays[14]. Observation of these decays might also provide new opportunities for calculating V_{bt} and V_{ts} ; the elements of the Cabibbo-Kobayashi-Maskawa (CKM) matrix. Recently, some studies on $B \rightarrow K_1(1270, 1400)\ell^+\ell^-$ decays have been made[15–23]. Theoretical studies of the decays into final states containing $K_1(1270, 1400)$ axial vector states is rendered more complicated due to the presence of K_1 mixing. The properties of axial vector states are studied in [24]. In QCD, the real physical axial vector K_1 states, $K_1(1270)$ and $K_1(1400)$ are mixtures of ideal $1^3P_1(K_{1A})$ and $1^1P_1(K_{1B})$ orbital angular momentum states, and their mixing is given as

$$\begin{pmatrix} |K_1(1270)\rangle \\ |K_1(1400)\rangle \end{pmatrix} = \mathcal{M}_\theta \begin{pmatrix} |K_{1A}\rangle \\ |K_{1B}\rangle \end{pmatrix}, \quad (2)$$

where

$$\mathcal{M}_\theta = \begin{pmatrix} \sin \theta_{K_1} & \cos \theta_{K_1} \\ \cos \theta_{K_1} & -\sin \theta_{K_1} \end{pmatrix} \quad (3)$$

is the mixing matrix, and θ_{K_1} is the mixing angle[25]. The magnitude of the mixing angle is estimated to be $34^\circ \leq |\theta_{K_1}| \leq 58^\circ$ [25, 27, 28]. More recently, the sign of θ_{K_1} , and a new window for the value of θ_{K_1} is estimated from the results of $B \rightarrow K_1(1270)\gamma$ and $\tau \rightarrow K_1(1270)\nu_\tau$ data as[16]

$$\theta_{K_1} = -(34 \pm 13)^\circ. \quad (4)$$

In this study, the results of [16] is used. Recently, the properties of low lying meson poles are analyzed in [26], indicating that there might be two meson poles corresponding to pseudo scalar $K_1(1270)$ states. In this work we assume the quark model picture, where there is only one pole, and no space for a second pole.

In this work, we calculate the transition form factors of $B \rightarrow K_1(1270, 1400)\ell^+\ell^-$ decays using three-point QCD sum rules approach. We also estimate the branching fractions for these decays, with the final leptons being e^+e^- , $\mu^+\mu^-$ and $\tau^+\tau^-$, and compare our results with the ones in the literature.

This paper is organized as follows. In section 2, the effective Hamiltonian for $B \rightarrow K_1(1270, 1400)\ell^+\ell^-$ decays are defined. The sum rules for these decays are derived in section 3. The explicit expressions for the form factors are also presented in section 3. In section 4, the numerical analysis of the results, the estimated branching fractions, and also the final discussions and remarks on the results are given.

II. DEFINING $B \rightarrow K_1(1270, 1400)\ell^+\ell^-$ TRANSITIONS

In SM the $B \rightarrow K_1\ell^+\ell^-$ transitions occur via $b \rightarrow s\ell^+\ell^-$ loop transition, due to penguin and box diagrams shown in Fig. 1. The effective Hamiltonian for $b \rightarrow s\ell^+\ell^-$ transition is written as[17]

$$\begin{aligned} \mathcal{H} = \frac{G_F\alpha}{2\sqrt{2}\pi} V_{tb}V_{ts}^* \times & \left\{ C_9^{eff} \bar{s}\gamma_\mu(1-\gamma_5)b\bar{l}\gamma_\mu l \right. \\ & + C_{10}\bar{s}\gamma_\mu(1-\gamma_5)b\bar{l}\gamma_\mu\gamma_5 l \\ & \left. - 2C_7^{eff} \frac{m^b}{q^2} \bar{s}\sigma_{\mu\nu}q^\nu(1+\gamma_5)b\bar{l}\gamma_\mu l \right\}, \end{aligned} \quad (5)$$

where C_7^{eff} , C_9^{eff} and C_{10} are the Wilson coefficients, G_F is the Fermi constant, α is the fine structure constant at the Z scale, V_{ij} are the elements of the CKM matrix and $q = p - p'$ is the momentum transferred to leptons. By sandwiching the effective Hamiltonian in Eq. 5 between initial and final meson states, the transition amplitude for $B \rightarrow K_1\ell^+\ell^-$ decays is obtained as

$$\begin{aligned} \mathcal{M} = \frac{G_F\alpha}{2\sqrt{2}\pi} V_{tb}V_{ts}^* \times & \left\{ C_9^{eff} \langle K_1(p', \epsilon) | \bar{s}\gamma_\mu(1-\gamma_5)b | B(p) \rangle \bar{l}\gamma_\mu l \right. \\ & + C_{10} \langle K_1(p', \epsilon) | \bar{s}\gamma_\mu(1-\gamma_5)b | B(p) \rangle \bar{l}\gamma_\mu\gamma_5 l \\ & \left. - 2C_7^{eff} \frac{m^b}{q^2} \langle K_1(p', \epsilon) | \bar{s}\sigma_{\mu\nu}q^\nu(1+\gamma_5)b | B(p) \rangle \bar{l}\gamma_\mu l \right\}, \end{aligned} \quad (6)$$

where $p(p')$ is the momentum of the $B(K_1)$ meson, and ϵ is the polarization vector of the axial vector K_1 meson. In order to calculate the amplitude, the matrix elements in Eq. 6 should be found. These matrix elements are parameterized in terms of the form factors as

$$\begin{aligned} \langle K_1(p', \epsilon) | \bar{s}\gamma_\mu(1-\gamma_5)b | B(p) \rangle = & \frac{2iA(q^2)}{M+m} \varepsilon_{\mu\nu\alpha\beta} \epsilon^{*\nu} p^\alpha p'^\beta - V_1 q^2 (M+m) \epsilon_\mu^* \\ & + \frac{V_2(q^2)}{M+m} (\epsilon^* \cdot p) P_\mu + \frac{V_3(q^2)}{M+m} (\epsilon^* \cdot p) q_\mu, \end{aligned} \quad (7)$$

$$\begin{aligned}
\langle K_1(p', \epsilon) | \bar{s} \sigma_{\mu\nu} q^\nu (1 + \gamma_5) b | B(p) \rangle &= 2T_1(q^2) \varepsilon_{\mu\nu\alpha\beta} \epsilon^{*\nu} p^\alpha p'^\beta \\
&- iT_2(q^2) [(M^2 - m^2) \epsilon_\mu^* - (\epsilon^* \cdot p) P_\mu] \\
&- iT_3(q^2) (\epsilon^* \cdot p) \left[q_\mu - \frac{q^2 P_\mu}{M^2 - m^2} \right], \tag{8}
\end{aligned}$$

where $P = p + p'$, $M \equiv M_B$, the mass of the B meson and $m \equiv m_{K_1}$ is the mass of the K_1 meson. The Dirac identity

$$\sigma_{\mu\nu} \gamma_5 = \frac{-i}{2} \varepsilon_{\mu\nu\alpha\beta} \sigma_{\alpha\beta} \tag{9}$$

with the convention $\gamma_5 = i\gamma_0\gamma_1\gamma_2\gamma_3$ and $\varepsilon_{0123} = -1$ requires that $T_1(0) = T_2(0)$. The relation of the chosen form factors with the ones in the literature [16, 17, 25] are presented in table I.

TABLE I: The relation of form factors used in this work, and used in literature[16, 17, 25].

this work	[16]	[17]	[25]
A	A	$g(M + m)$	
V_1	V_1	$f/(M + m)$	
V_2	V_2	$-a_+(M + m)$	
V_3	$\frac{-2m(M+m)}{q^2}(V_3 - V_0)$	$-a_-(M + m)$	
T_1	T_1	$-g_+$	$-Y_1/2$
T_2	T_2	$-g_+ - g_- \frac{q^2}{M+m}$	Y_2
T_3	T_3	$g_- + h(M + m)$	Y_2

In this work the branching fractions of $B \rightarrow K_1(1270, 1400)\ell^+\ell^-$ transitions are also estimated. The partial decay width of the B meson is found by squaring the amplitude in Eq. 6, and by multiplying the phase space factors as

$$\frac{d\Gamma}{d\hat{q}} = \frac{G_F^2 \alpha^2 M}{2^{14} \pi^5} |V_{tb} V_{ts}^*|^2 \lambda^{1/2}(1, \hat{r}, \hat{q}) v \Delta(\hat{q}), \tag{10}$$

where $\hat{q} = q^2/M^2$, $\lambda(a, b, c) = a^2 + b^2 + c^2 - 2(ab + bc + ca)$ and

$$\begin{aligned}
\Delta(\hat{q}) &= \frac{2}{3\hat{r}\hat{q}} M^2 \text{Re} \left[-12M^2 \hat{m}_l \hat{q} \lambda(1, \hat{r}, \hat{q}) \left\{ (\mathcal{E}_3 - \mathcal{D}_2 - \mathcal{D}_3) \mathcal{E}_1^* \right. \right. \\
&- (\mathcal{E}_2 + \mathcal{E}_3 - \mathcal{D}_3) \mathcal{D}_1^* \left. \left. \right\} + 12M^4 \hat{m}_l \hat{q} (1 - \hat{r}) \lambda(1, \hat{r}, \hat{q}) (\mathcal{E}_2 - \mathcal{D}_2) (\mathcal{E}_3^* - \mathcal{D}_3^*) \right. \\
&+ 48\hat{m}_l \hat{r} \hat{q} \left\{ 3\mathcal{E}_1 \mathcal{D}_1^* + 2M^4 \lambda(1, \hat{r}, \hat{q}) \mathcal{E}_0 \mathcal{D}_0^* \right\} - 16M^4 \hat{r} \hat{q} (\hat{m}_l - \hat{q}) \lambda(1, \hat{r}, \hat{q}) \left\{ |\mathcal{E}_0|^2 + |\mathcal{D}_0|^2 \right\} \\
&- 6M^4 \hat{m}_l \hat{q} \lambda(1, \hat{r}, \hat{q}) \left\{ 2(2 + 2\hat{r} - \hat{q}) \mathcal{E}_2 \mathcal{D}_2^* - \hat{q} |(\mathcal{E}_3 - \mathcal{D}_3)|^2 \right\} \\
&- 4M^2 \lambda(1, \hat{r}, \hat{q}) \left\{ \hat{m}_l (2 - 2\hat{r} + \hat{q}) + \hat{q} (1 - \hat{r} - \hat{q}) \right\} (\mathcal{E}_1 \mathcal{E}_2^* + \mathcal{D}_1 \mathcal{D}_2^*) \\
&+ \hat{q} \left\{ 6\hat{r} \hat{q} (3 + v^2) + \lambda(1, \hat{r}, \hat{q}) (3 - v^2) \right\} \left\{ |\mathcal{E}_1|^2 + |\mathcal{D}_1|^2 \right\} \\
&- 2M^4 \lambda(1, \hat{r}, \hat{q}) \left\{ \hat{m}_l [\lambda(1, \hat{r}, \hat{q}) - 3(1 - \hat{r})^2] - \lambda(1, \hat{r}, \hat{q}) \hat{q} \right\} \left\{ |\mathcal{E}_2|^2 + |\mathcal{D}_2|^2 \right\} \right], \tag{11}
\end{aligned}$$

and $\hat{r} = m^2/M^2$, $\hat{m}_l = m_l^2/M^2$ and $v = \sqrt{1 - 4\hat{m}_l/\hat{q}}$ is the final lepton velocity. The following definitions are also used.

$$\mathcal{D}_0 = (C_9^{eff} + C_{10}) \frac{A(q^2)}{M + m} + (2m_b C_7^{eff}) \frac{T_1(q^2)}{q^2},$$

$$\begin{aligned}
\mathcal{D}_1 &= (C_9^{eff} + C_{10})(M + m)V_1(q^2) + (2m_b C_7^{eff})(M^2 - m^2)\frac{T_2(q^2)}{q^2}, \\
\mathcal{D}_2 &= \frac{C_9^{eff} + C_{10}}{M + m}V_2(q^2) + (2m_b C_7^{eff})\frac{1}{q^2}\left[T_2(q^2) + \frac{q^2}{M^2 - m^2}T_3(q^2)\right], \\
\mathcal{D}_3 &= (C_9^{eff} + C_{10})\frac{V_3(q^2)}{M + m} - (2m_b C_7^{eff})\frac{T_3(q^2)}{q^2}, \\
\mathcal{E}_0 &= (C_9^{eff} - C_{10})\frac{A(q^2)}{M + m} + (2m_b C_7^{eff})\frac{T_3(q^2)}{q^2}, \\
\mathcal{E}_1 &= (C_9^{eff} - C_{10})(M + m)V_1(q^2) + (2m_b C_7^{eff})(M^2 - m^2)\frac{T_2(q^2)}{q^2}, \\
\mathcal{E}_2 &= \frac{C_9^{eff} - C_{10}}{M + m}V_2(q^2) + (2m_b C_7^{eff})\frac{1}{q^2}\left[T_2(q^2) + \frac{q^2}{M^2 - m^2}T_3(q^2)\right], \\
\mathcal{E}_3 &= (C_9^{eff} - C_{10})\frac{V_3(q^2)}{M + m} - (2m_b C_7^{eff})\frac{T_3(q^2)}{q^2}.
\end{aligned} \tag{12}$$

III. SUM RULES FOR $B \rightarrow K_1(1270, 1400)\ell^+\ell^-$ TRANSITIONS

In this section the sum rules for the form factors of $B \rightarrow K_1(1270, 1400)\ell^+\ell^-$ transitions are found. In QCD sum rules approach, to obtain the matrix elements in Eqs. 7 and 8, one can start from the three-point correlation functions

$$\begin{aligned}
\Pi_{\mu\nu}^{A,a}(p^2, p'^2) &= i^2 \int dx^4 dy^4 e^{-ipx} e^{ip'y} \langle 0 | T [J_\nu^A(y) J_\mu^a(0) J_B^\dagger(x)] | 0 \rangle, \\
\Pi_{\mu\nu\rho}^{T,a}(p^2, p'^2) &= i^2 \int dx^4 dy^4 e^{-ipx} e^{ip'y} \langle 0 | T [J_{\nu\rho}^T(y) J_\mu^a(0) J_B^\dagger(x)] | 0 \rangle,
\end{aligned} \tag{13}$$

where $J_\nu^A = \bar{s}\gamma_\nu\gamma_5 d$ and $J_{\nu\rho}^T = \bar{s}\sigma_{\nu\rho}\gamma_5 d$ are axial vector and tensor interpolating currents creating K_1 states, $J_B = \bar{b}\gamma_5 d$ is the interpolating current of B mesons, and $J_\mu^a = J_\mu^{V-A, T+PT}$ are the vector and tensor parts of the transition currents with $J_\mu^{V-A} = \bar{b}\gamma_\mu(1 - \gamma_5)s$ and $J^{T+PT} = \bar{b}\sigma_{\mu\rho}q^\rho(1 + \gamma_5)s$.

The correlators are calculated in the following way. First, they are saturated with two complete sets of intermediate states with same quantum numbers of the initial and final state currents. These calculations in terms of the matrix elements of $K_1(1270)$ and $K_1(1400)$ states form the phenomenological part of the QCD sum rules. The phenomenological parts of the correlators (Eq. 13) can be written as

$$\begin{aligned}
\Pi_{\mu\nu}^{A,a}(p^2, p'^2) &= -\frac{\langle 0 | J_\nu^A | K_1(1270)(p', \epsilon) \rangle \langle K_1(1270)(p', \epsilon) | J_\mu^a | B(p) \rangle \langle B(p) | J_B | 0 \rangle}{R_1 R} \\
&\quad - \frac{\langle 0 | J_\nu^A | K_1(1400)(p', \epsilon) \rangle \langle K_1(1400)(p', \epsilon) | J_\mu^a | B(p) \rangle \langle B(p) | J_B | 0 \rangle}{R_2 R} \\
&\quad + \text{higher resonances and continuum states,} \\
\Pi_{\mu\nu\rho}^{T,a}(p^2, p'^2) &= -\frac{\langle 0 | J_{\nu\rho}^T | K_1(1270)(p', \epsilon) \rangle \langle K_1(1270)(p', \epsilon) | J_\mu^a | B(p) \rangle \langle B(p) | J_B | 0 \rangle}{R_1 R} \\
&\quad - \frac{\langle 0 | J_{\nu\rho}^T | K_1(1400)(p', \epsilon) \rangle \langle K_1(1400)(p', \epsilon) | J_\mu^a | B(p) \rangle \langle B(p) | J_B | 0 \rangle}{R_2 R} \\
&\quad + \text{higher resonances and continuum states,}
\end{aligned} \tag{14}$$

where $R = p^2 - M^2$, $R_1 = p'^2 - m_{K_1(1270)}^2$ and $R_2 = p'^2 - m_{K_1(1400)}^2$. The matrix elements for the B meson is defined as

$$\langle B(p) | J_B | 0 \rangle = -i \frac{F_B M^2}{m_b + m_d}. \tag{15}$$

In QCD sum rules, each correlator function has its own continuum. Due to this fact, obtaining the matrix elements $\langle K_1(1270)(p', \epsilon) | J_\mu^a | B(p) \rangle$ and $\langle K_1(1400)(p', \epsilon) | J_\mu^a | B(p) \rangle$ from two correlator reduces the reliability of the sum rules. An alternative way to obtain the transition matrix elements is to express $K_1(1400)$ and $K_1(1270)$ states in terms of K_{1A} and K_{1B} which are G-parity eigenstates as defined in Eq. 2[15, 16]. In this work, G-parity is used as a generalization of C parity defined for $q\bar{q}$ mesons to $qq\bar{q}$ multiplets as done in[15].

The matrix elements $\langle K_1(1270) | J_\mu | B \rangle$ and $\langle K_1(1400) | J_\mu | B \rangle$ in Eq. 6 can be written in terms of matrix elements $\langle K_{1A} | J_\mu | B \rangle$ and $\langle K_{1B} | J_\mu | B \rangle$ states as[24]

$$\begin{pmatrix} \langle K_1(1270) | J_\mu | B \rangle \\ \langle K_1(1400) | J_\mu | B \rangle \end{pmatrix} = \mathcal{M}_\theta \begin{pmatrix} \langle K_{1A} | J_\mu | B \rangle \\ \langle K_{1B} | J_\mu | B \rangle \end{pmatrix} \quad (16)$$

where J_μ are any of the transition currents. Due to this relation, the form factors parameterizing $\langle K_1(1270, 1400) | J_\mu | B \rangle$ matrix elements can be expressed in terms of the form factors parameterizing $\langle K_{1(A,B)} | J_\mu | B \rangle$ matrix elements as follows

$$\begin{pmatrix} \xi f_i^{1270} \\ \xi' f_i^{1400} \end{pmatrix} = \mathcal{M}_\theta \begin{pmatrix} \varsigma f_{i,A} \\ \varsigma' f_{i,B} \end{pmatrix} \quad (17)$$

where f_i is defined as the form factors $\{A, V_1, V_2, V_3, T_1, T_2, T_3\}$ respectively for $i = 1, 2, \dots, 7$, and f_i^{1270} , f_i^{1400} , $f_{i,A}$ and $f_{i,B}$ denotes the form factors parameterizing $\langle K_1(1270) | J_\mu | B \rangle$, $\langle K_1(1400) | J_\mu | B \rangle$, $\langle K_{1A} | J_\mu | B \rangle$ and $\langle K_{1B} | J_\mu | B \rangle$ matrix elements respectively. The values for factors ξ , ξ' , ς and ς' are given in table II, where $m_1 \equiv m_{K_1(1270)}$, $m_2 \equiv m_{K_1(1400)}$, $m_A \equiv m_{K_{1A}}$ and $m_B \equiv m_{K_{1B}}$. The masses of K_{1A} and K_{1B} states are defined as[16]

$$\begin{aligned} m_{K_{1A}}^2 &= m_{K_1(1400)}^2 \cos^2 \theta_K + m_{K_1(1270)}^2 \sin^2 \theta_K \\ m_{K_{1B}}^2 &= m_{K_1(1400)}^2 \sin^2 \theta_K + m_{K_1(1270)}^2 \cos^2 \theta_K. \end{aligned} \quad (18)$$

TABLE II: The values for factors ξ , ξ' , ς and ς' for the form factors.

f_i	ξ	ξ'	ς	ς'
A, V_2, V_3	$1/(M + m_1)$	$1/(M + m_2)$	$1/(M + m_A)$	$1/(M + m_B)$
V_1	$(M + m_1)$	$(M + m_2)$	$(M + m_A)$	$(M + m_B)$
T_1, T_3	1	1	1	1
T_2	$(M^2 - m_1^2)$	$(M^2 - m_2^2)$	$(M^2 - m_A^2)$	$(M^2 - m_B^2)$

Inserting Eqs. 2 and 16 in Eq. 14, and applying double Borel transformations, the phenomenological parts of the correlators are found in terms of G-parity eigen states as

$$\begin{aligned} \hat{\Pi}_{\mu\nu}^{A,a}(p^2, p'^2) &= -e^{-\frac{-M^2}{M_1^2}} e^{-\frac{-m_1^2}{M_2^2}} \left\{ \langle 0 | J_\nu^A \left[s^2 |K_{1A}(p', \epsilon)\rangle \langle K_{1A}(p', \epsilon)| + c^2 |K_{1B}(p', \epsilon)\rangle \langle K_{1B}(p', \epsilon)| \right. \right. \\ &\quad \left. \left. + sc \left(|K_{1A}(p', \epsilon)\rangle \langle K_{1B}(p', \epsilon)| + |K_{1B}(p', \epsilon)\rangle \langle K_{1A}(p', \epsilon)| \right) \right] J_\mu^a | B(p) \rangle \langle B(p) | J_B | 0 \rangle \right\} \\ &\quad - e^{-\frac{-M^2}{M_1^2}} e^{-\frac{-m_2^2}{M_2^2}} \left\{ \langle 0 | J_\nu^A \left[c^2 |K_{1A}(p', \epsilon)\rangle \langle K_{1A}(p', \epsilon)| + s^2 |K_{1B}(p', \epsilon)\rangle \langle K_{1B}(p', \epsilon)| \right. \right. \\ &\quad \left. \left. + sc \left(|K_{1A}(p', \epsilon)\rangle \langle K_{1B}(p', \epsilon)| + |K_{1B}(p', \epsilon)\rangle \langle K_{1A}(p', \epsilon)| \right) \right] J_\mu^a | B(p) \rangle \langle B(p) | J_B | 0 \rangle \right\} \end{aligned}$$

$$\begin{aligned}
& -sc \left(|K_{1A}(p', \epsilon)\rangle\langle K_{1B}(p', \epsilon)| + |K_{1B}(p', \epsilon)\rangle\langle K_{1A}(p', \epsilon)| \right) \left. J_\mu^a |B(p)\rangle\langle B(p)|J_B|0\rangle \right\} \\
\hat{\Pi}_{\mu\nu\rho}^{T,a}(p^2, p'^2) = & -e^{-\frac{-M^2}{M_1^2}} e^{-\frac{-m_1^2}{M_2^2}} \left\{ \langle 0|J_{\nu\rho}^T \left[s^2 |K_{1A}(p', \epsilon)\rangle\langle K_{1A}(p', \epsilon)| + c^2 |K_{1B}(p', \epsilon)\rangle\langle K_{1B}(p', \epsilon)| \right. \right. \\
& + sc \left(|K_{1A}(p', \epsilon)\rangle\langle K_{1B}(p', \epsilon)| + |K_{1B}(p', \epsilon)\rangle\langle K_{1A}(p', \epsilon)| \right) \left. \left. J_\mu^a |B(p)\rangle\langle B(p)|J_B|0\rangle \right\} \\
& -e^{-\frac{-M^2}{M_1^2}} e^{-\frac{-m_2^2}{M_2^2}} \left\{ \langle 0|J_{\nu\rho}^T \left[c^2 |K_{1A}(p', \epsilon)\rangle\langle K_{1A}(p', \epsilon)| + s^2 |K_{1B}(p', \epsilon)\rangle\langle K_{1B}(p', \epsilon)| \right. \right. \\
& -sc \left(|K_{1A}(p', \epsilon)\rangle\langle K_{1B}(p', \epsilon)| + |K_{1B}(p', \epsilon)\rangle\langle K_{1A}(p', \epsilon)| \right) \left. \left. J_\mu^a |B(p)\rangle\langle B(p)|J_B|0\rangle \right\},
\end{aligned} \tag{19}$$

where $s \equiv \sin \theta_{K_1}$ and $c \equiv \cos \theta_{K_1}$. M_1^2 and M_2^2 appearing in Eq. 19 are Borel mass parameters and $\hat{\Pi}$ denotes the Borel transformation of Π . The double Borel transformation with respect to the variables p^2 and p'^2 ($p^2 \rightarrow M_1^2, p'^2 \rightarrow M_2^2$) is given as

$$\hat{\mathcal{B}} \left[\frac{1}{(p^2 - m_1^2)^m} \frac{1}{(p'^2 - m_2^2)^n} \right] \rightarrow (-1)^{m+n} \frac{1}{\Gamma(m)} \frac{1}{\Gamma(n)} e^{-m_1^2/M_1^2} e^{-m_2^2/M_2^2} \frac{1}{(M_1^2)^{m-1} (M_2^2)^{n-1}}. \tag{20}$$

The matrix elements of $K_{1(A,B)}$ states are defined in terms of both G parity conserving and violating decay constants discussed in [24]. The G parity conserving decay constants are given as

$$\begin{aligned}
\langle K_{1A}(p', \epsilon) | \bar{s} \gamma_\mu \gamma_5 d | 0 \rangle &= i f_{K_{1A}} m_A \epsilon_\mu^*, \\
\langle K_{1B}(p', \epsilon) | \bar{s} \sigma_{\mu\nu} \gamma_5 d | 0 \rangle &= f_{K_{1B}}^\perp [\epsilon_\mu^* p'_\nu - \epsilon_\nu^* p'_\mu],
\end{aligned} \tag{21}$$

and the G parity violating decay constants are given as

$$\begin{aligned}
\langle K_{1A}(p', \epsilon) | \bar{s} \sigma_{\mu\nu} \gamma_5 d | 0 \rangle &= i f_{K_{1A}} a_0^{\perp K_{1A}} [\epsilon_\mu^* p'_\nu - \epsilon_\nu^* p'_\mu], \\
\langle K_{1B}(p', \epsilon) | \bar{s} \gamma_\mu \gamma_5 d | 0 \rangle &= i f_{K_{1B}}^\perp m_B (1 \text{ GeV}) a_0^{\parallel K_{1B}} \epsilon_\mu^*,
\end{aligned} \tag{22}$$

where $f_{K_{1A}} (\equiv f_A)$ and $f_{K_{1B}}^\perp (\equiv f_B)$ are the decay constants of K_{1A} and K_{1B} mesons, and $a_0^{\perp K_{1A}}$ and $a_0^{\parallel K_{1B}}$ are the zeroth Gegenbauer moments. Since the Gegenbauer moments are zero in $SU(3)$ limit [15], the G parity violating matrix elements are expected to be small. In [24], their values are predicted to be consistent with zero. In this work, they will be neglected. After defining the matrix elements $\langle K_{1(A,B)} | J_\mu | B \rangle$ and inserting in Eq. 19 the following assumptions are made.

$$\begin{aligned}
& e^{-\frac{-m_1^2}{M_2^2}} s^2 |K_{1A}(p', \epsilon)\rangle\langle K_{1A}(p', \epsilon)| + e^{-\frac{-m_2^2}{M_2^2}} c^2 |K_{1A}(p', \epsilon)\rangle\langle K_{1A}(p', \epsilon)| \sim e^{-\frac{-m_A^2}{M_2^2}} |K_{1A}(p', \epsilon)\rangle\langle K_{1A}(p', \epsilon)| \\
& e^{-\frac{-m_1^2}{M_2^2}} c^2 |K_{1B}(p', \epsilon)\rangle\langle K_{1B}(p', \epsilon)| + e^{-\frac{-m_2^2}{M_2^2}} s^2 |K_{1B}(p', \epsilon)\rangle\langle K_{1B}(p', \epsilon)| \sim e^{-\frac{-m_B^2}{M_2^2}} |K_{1B}(p', \epsilon)\rangle\langle K_{1B}(p', \epsilon)| \\
& \left(e^{-\frac{-m_1^2}{M_2^2}} - e^{-\frac{-m_2^2}{M_2^2}} \right) sc \left(|K_{1A}(p', \epsilon)\rangle\langle K_{1B}(p', \epsilon)| + |K_{1B}(p', \epsilon)\rangle\langle K_{1A}(p', \epsilon)| \right) \sim 0.
\end{aligned} \tag{23}$$

The numerical values of the masses of K_1 states given in numerical discussions satisfy $m_1 < m_A < m_B < m_2$. And also the minimum value of the Borel mass parameter M_2^2 guarantees $e^{-\frac{-m_1^2 + m_2^2}{M_2^2}} > 0.94$. Due to this considerations the assumptions made in Eq. 23 effects the results of the form factors by less than 3%. After employing the assumptions defined in Eq. 23, the phenomenological parts of the correlators are written in terms of G-parity eigenstates as

$$\begin{aligned}
\hat{\Pi}_{\mu\nu}^{A,a}(p^2, p'^2) &= -e^{-\frac{-M^2}{M_1^2}} e^{-\frac{-m_A^2}{M_2^2}} \langle 0 | J_\nu^A | K_{1A}(p', \epsilon) \rangle \langle K_{1A}(p', \epsilon) | J_\mu^a | B(p) \rangle \langle B(p) | J_B | 0 \rangle \\
\hat{\Pi}_{\mu\nu\rho}^{T,a}(p^2, p'^2) &= -e^{-\frac{-M^2}{M_1^2}} e^{-\frac{-m_B^2}{M_2^2}} \langle 0 | J_{\nu\rho}^T | K_{1B}(p', \epsilon) \rangle \langle K_{1B}(p', \epsilon) | J_\mu^a | B(p) \rangle \langle B(p) | J_B | 0 \rangle.
\end{aligned} \tag{24}$$

Using equations 15, 21 and 24 and summing over the polarizations of the $K_{1(A,B)}$ mesons, the so called phenomenological parts of the correlation functions are found and expressed in terms of selected structures as

$$\begin{aligned}
\hat{\Pi}_{\mu\nu}^{A(V-A)} &= \frac{F_B M^2}{m_b + m_c} f_A m_A e^{\frac{-M^2}{M_1^2}} e^{\frac{-m_A^2}{M_2^2}} \left[g_{\mu\nu} A_A (M + m_A) \right. \\
&\quad + \frac{1}{2} V_{2A} (M + m_A) (p_\mu p_\nu + p'_\mu p'_\nu) \\
&\quad + \frac{1}{2} V_{3A} (M + m_A) (p_\mu p_\nu - p'_\mu p'_\nu) \\
&\quad \left. + i \frac{V_{1A} \varepsilon_{\mu\nu\rho\ell} p^\rho p'^\ell}{(M + m_A)} \right], \\
\hat{\Pi}_{\mu\nu}^{A(T+PT)} &= \frac{F_B M^2}{m_b + m_c} f_A m_A e^{\frac{-M^2}{M_1^2}} e^{\frac{-m_A^2}{M_2^2}} \left[iT_{1A} \varepsilon_{\mu\nu\rho\ell} p^\rho p'^\ell \right. \\
&\quad \left. + \frac{T_{2A} g_{\mu\nu}}{M^2 - m_A^2} + T_{3A} (p_\mu p_\nu + p'_\mu p'_\nu) / 2 \right],
\end{aligned} \tag{25}$$

and

$$\begin{aligned}
\hat{\Pi}_{\mu\nu\rho}^{T(V-A)} &= i \frac{F_B M^2}{m_b + m_c} f_B e^{\frac{-M^2}{M_1^2}} e^{\frac{-m_B^2}{M_2^2}} \left[A_B (M + m_B) g_{\mu\nu} p'_\rho \right. \\
&\quad + \frac{1}{2} V_{2B} (M + m_B) (p_\mu p_\nu + p'_\mu p'_\nu) p_\rho \\
&\quad + \frac{1}{2} V_{3B} (M + m_B) (p_\mu p_\nu - p'_\mu p'_\nu) p_\rho \\
&\quad \left. + i \frac{V_{1B} \varepsilon_{\mu\nu\alpha\ell} p^\alpha p'^\ell p_\rho}{(M + m_B)} \right], \\
\hat{\Pi}_{\mu\nu\rho}^{T(T+PT)} &= \frac{F_B M^2}{m_b + m_c} f_B e^{\frac{-M^2}{M_1^2}} e^{\frac{-m_B^2}{M_2^2}} \left[i \frac{1}{2} T_{1B} \varepsilon_{\mu\nu\alpha\ell} p^\alpha p'^\ell p_\rho \right. \\
&\quad + \frac{T_{2B} g_{\mu\nu} p_\rho}{(M^2 - m_B^2)} \\
&\quad \left. + \frac{1}{2} T_{3B} (p_\mu p_\nu + p'_\mu p'_\nu) p_\rho \right].
\end{aligned} \tag{26}$$

In QCD sum rules, the correlation functions are also calculated theoretically using the operator product expansion (OPE) in the space-like region where $p^2 \ll (m_s + m_d)^2$ and $p^2 \ll (m_b + m_d)^2$ in the so called deep Euclidean region. The contributions to the correlation functions in the QCD side of sum rules come from bare-loop (perturbative) diagrams and also quark condensates (nonperturbative). The correlators can be written as

$$\begin{aligned}
\hat{\Pi}_{\mu\nu}^{A(V-A)} &= \hat{\Pi}_{A_A} g_{\mu\nu} \\
&\quad + \frac{\hat{\Pi}_{V_{2A}} (p_\mu p_\nu + p'_\mu p'_\nu)}{2} + \frac{\hat{\Pi}_{V_{3A}} (p_\mu p_\nu - p'_\mu p'_\nu)}{2} \\
&\quad + i \hat{\Pi}_{V_{1A}} \varepsilon_{\mu\nu\rho\ell} p^\rho p'^\ell, \\
\hat{\Pi}_{\mu\nu}^{A(T+PT)} &= \hat{\Pi}_{T_{1A}} \varepsilon_{\mu\nu\rho\ell} p^\rho p'^\ell + \hat{\Pi}_{T_{2A}} g_{\mu\nu} \\
&\quad + \hat{\Pi}_{T_{3A}} \frac{(p_\mu p_\nu + p'_\mu p'_\nu)}{2},
\end{aligned} \tag{27}$$

and

$$\hat{\Pi}_{\mu\nu\rho}^{T(V-A)} = i \hat{\Pi}_{V_{2B}} \frac{(p_\mu p_\nu + p'_\mu p'_\nu) p_\rho}{2}$$

$$\begin{aligned}
& + \frac{\hat{\Pi}_{V_{3B}}(p_\mu p_\nu - p'_\mu p'_\nu)p_\rho}{2} \\
& + \hat{\Pi}_{A_B} g_{\mu\nu} p'_\rho + i \hat{\Pi}_{V_{1B}} \varepsilon_{\mu\nu\alpha\beta} p^\alpha p'^\beta p_\rho, \\
\hat{\Pi}_{\mu\nu\rho}^{T(T+PT)} = & i \frac{\hat{\Pi}_{T_{1B}} \varepsilon_{\mu\nu\alpha\beta} p^\alpha p'^\beta p_\rho}{2} \\
& + \hat{\Pi}_{T_{2B}} g_{\mu\nu} p_\rho \\
& + \frac{\hat{\Pi}_{T_{3B}}(p_\mu p_\nu + p'_\mu p'_\nu)p_\rho}{2}.
\end{aligned} \tag{28}$$

Each of $\hat{\Pi}_{f_i(A,B)}$ are expressed in terms of perturbative and nonperturbative contributions as

$$\hat{\Pi}_{f_i(A,B)} = \hat{\Pi}_{f_i(A,B)}^{pert} + \hat{\Pi}_{f_i(A,B)}^{nonpert}. \tag{29}$$

The perturbative parts of the correlators are written in terms of double dispersion relation for the coefficients of the selected Lorentz structures, as

$$\hat{\Pi}_{f_i}^{per} = \int ds \int ds' \rho_{f_i}(s, s', q^2) e^{\frac{-s}{M^2}} e^{\frac{-s'}{M^2}}, \tag{30}$$

where $\rho_{f_i}(s, s', q^2)$ are the spectral densities defined as

$$\rho_{f_i}(s, s'; q^2) = \frac{Im_s Im_{s'} \Pi_{f_i}^{OPE}(s, s'; q^2)}{\pi^2}. \tag{31}$$

The spectral densities in Eq. 30 are calculated by using the usual Feynman integral for the loop diagrams, with the help of Cutkovsky rules, i.e., by inserting delta functions instead of the quark propagators ($\frac{1}{p^2 - m^2} \rightarrow 2i\pi\delta(p^2 - m^2)$), implying that all quarks are real. The physical region in s, s' plane is described by the following inequality

$$-1 \leq f(s, s') = \frac{2ss' + (m_b^2 - s - m_d^2)(s + s' - q^2) + 2s(m_b^2 - m_d^2)}{\lambda^{1/2}(m_b^2, s, m_d^2)\lambda^{1/2}(s, s', q^2)} \leq +1. \tag{32}$$

The calculations lead to the following results for the spectral densities. For the $\langle K_{1A} | J_\mu | B \rangle$ matrix elements, the spectral densities are calculated as

$$\rho_{A_A} = 2(M + m)I_0\{m_d + (-m_b + m_d)A_1 + (m_d + m_s)B_1\}, \tag{33}$$

$$\begin{aligned}
\rho_{V_{1A}} = & \frac{2}{M + m} I_0\{m_d[(m_d - m_b)(m_d + m_s) - q^2 + s + s'] \\
& + [2m_s s + m_b(q^2 - s - s') + m_d(-q^2 + 3s + s')]\}A_1 + 4(m_b - m_d)A_2 \\
& + [(m_d + m_s)(s - q^2) + (m_s + 3m_d - 2m_b)]B_1\},
\end{aligned} \tag{34}$$

$$\rho_{V_{2A}} = 2(M + m)I_0\{m_d - (m_b - 3m_d)A_1 + (m_d + m_s)B_1 - 2(m_b - m_d)(B_2 + D_2)\}, \tag{35}$$

$$\rho_{V_{3A}} = -2(M + m)I_0\{m_d - (m_b + m_d)A_1 + (m_d + m_s)B_1 + 2(m_b - m_d)(B_2 - D_2)\}, \tag{36}$$

$$\begin{aligned}
\rho_{T_{1A}} = & -4e^{\frac{-s}{M^2}} e^{\frac{-s'}{M^2}} I_0\{m_d(m_s - m_b) + 6A_2 \\
& + [s + (m_d - m_s)(m_s + m_d)]A_1 + [s' + (m_d - m_s)(m_s + m_d)]B_1 \\
& + 2sB_2 - (q^2 - s)(C_2 + D_2) + s'(C_2 + D_2 + 2F_2)\}
\end{aligned} \tag{37}$$

$$\begin{aligned}
\rho_{T_{2A}} = & \frac{2}{M^2 - m^2} I_0\{-m_d[2m_d(s - s') + m_s(q^2 + s - s') + m_b(q^2 - s + s')] \\
& + [-m_d^2(q^2 + s - s') - m_d m_s(q^2 + s - s') + m_b(m_d + m_s)(q^2 + s - s') + s(q^2 - s + s')]A_1 \\
& + 2(q^2 + s - s')A_2 + [(m_d - m_b)(m_d + m_s)(q^2 - s + s') - (q^2 + s - s')s']B_1\},
\end{aligned} \tag{38}$$

$$\rho_{T_{3A}} = 2I_0\{m_d(2m_d - m_b + m_s) + [s + (m_d - m_b)(m_d + m_s)]A_1 - 2A_2 + [s' + (m_d - m_b)(m_d + m_s)]B_1 + 2q^2 D_2\}. \tag{39}$$

For the $\langle K_{1B}|J_\mu|B\rangle$ matrix elements, the spectral densities are calculated as

$$\rho_{AB} = -8(M+m)I_0(s, s', q^2)\{B_1 + D_2 + F_2\}, \quad (40)$$

$$\rho_{V_{1B}} = \frac{4}{M+m}I_0(s, s', q^2)\{(m_b - m_d)m_d - sA_1 + [(m_b - m_d)(m_d + m_s) + q^2 - s - s']B_1 - 2sD_2 + (q^2 - s - s')F_2\}, \quad (41)$$

$$\rho_{V_{2B}} = -4(M+m)I_0(s, s', q^2)\{B_1 + D_2 + F_2\}, \quad (42)$$

$$\rho_{V_{3B}} = 4(M+m)I_0(s, s', q^2)\{B_1 - D_2 + F_2\}, \quad (43)$$

$$\rho_{T_{1B}} = 8I_0(s, s', q^2)\{(m_b - m_s)(B_1 + D_2 + F_2)\}, \quad (44)$$

$$\rho_{T_{2B}} = \frac{-4}{M^2 - m^2}I_0(s, s', q^2)\{[s' + (m_d - m_b)(m_d + m_s) - 4(m_b - m_d)A_2] + [sm_s + s'm_b + m_d(q^2 - 2s')]A_1 + s'(m_b - 2m_d + m_s)B_1 + (m_d - m_b)(q^2 + s - s')B_2 + (m_b - m_d)(q^2 - s + s')C_2\}, \quad (45)$$

$$\rho_{T_{3B}} = -4I_0(s, s', q^2)\{m_d - (m_b - 2m_d)A_1 - 2(m_b - 2m_d)B_1 - (m_b - m_d)(B_2 + 2D_2 + F_2)\}, \quad (46)$$

where

$$I_0(s, s', q^2) = \frac{1}{\lambda^{\frac{1}{2}}(s, s', q^2)}, \quad (47)$$

$$A_1 = \frac{s'(q^2 + s - s' - 2m_b^2) + m_d^2(q^2 - s + s') + m_s^2(s + s' - q^2)}{q^4 - (s - s')^2 - 2q^2(s + s')}, \quad (48)$$

$$B_1 = \frac{s(q^2 - s + s' - 2m_s^2) + m_d^2(q^2 + s - s') + m_b^2(-s - s' + q^2)}{q^4 - (s - s')^2 - 2q^2(s + s')}, \quad (49)$$

$$A_2 = \frac{1}{2(q^4 - (s - s')^2 - 2q^2(s + s'))}\{m_d^4q^2 + m_b^4s' + s(m_s^4 + q^2s' - m_s^2(q^2 - s + s')) - m_b^2[s'(q^2 + s - s') + m_d^2(q^2 - s + s') + m_s^2(s + s' - q^2)] - m_d^2[m_s^2(q^2 + s - s') + q^2(-q^2 + s + s')]\}, \quad (50)$$

$$B_2 = \frac{1}{(q^4 - (s - s')^2 - 2q^2(s + s'))^2}\{m_s^4[q^4 + s^2 + 4ss' + s'^2 - 2q^2(s + s')] + s'^2[6m_b^4 + q^4 + 4sq^2 + s^2 - 6m_b^2(q^2 + s - s') - 2(q^2 + s)s' + s'^2] + m_d^4[(q^2 - s)^2 + 4q^2s' - 2ss' + s'^2] - 2m_s^2s'[q^4 - 2s^2 + q^2(s - 2s') + ss' + s'^2] + 3m_b^2(s + s' - q^2) - 2m_d^2[m_s^2((s - q^2)^2 + (s + q^2)s' - 2s'^2) + s'(-2q^4 + (s - s')^2 + 3m_b^2(q^2 - s + s') + q^2(s + s'))]\}, \quad (51)$$

$$C_2 = \frac{1}{(q^4 - (s - s')^2 - 2q^2(s + s'))^2}\{3m_b^4(q^2 - s - s')s' - 2m_b^2[(m_d^2 - m_s^2)(q^2 - s)^2 + 2m_s^2s'(q^2 - 2s) + s(m_d^2(q^2 + s) + (q^2 - s)(q^2 + 2s)) - s'^2(2m_d^2 + m_s^2 + 2q^2 - s) + s'^3] + m_d^4[2q^4 - (s - s')^2 - q^2(s + s')] - m_d^2[-q^6 + q^4(s + s') - (s - s')^2(s + s') + q^2(s^2 - 6ss' + s'^2) + 2m_s^2(q^4 - 2s^2 + q^2(s - 2s') + ss' + s'^2)] - s[3m_s^4(s + s' - q^2) + 2m_b^2((q^2 - s)^2 + (q^2 - s)s' - 2s'^2) + s'(-2q^4 + s - s'^2 + q^2(s + s'))]\}, \quad (52)$$

$$D_2 = C_2, \quad (53)$$

$$F_2 = \frac{1}{(q^4 - (s - s')^2 - 2q^2(s + s'))^2}\{m_d^4[q^4 + q^2s + s^2 - 2s'(q^2 - s) + s'^2] + s'^2[6m_s^4 + (q^2 - s)^2 + 4q^2s' - 2ss' + s'^2 - 6m_s^2(q^2 - s + s')] + m_b^4[q^4 + s^2 + 4ss' + s'^2 - 2q^2(s + s')] - 2m_d^2s[-2q^4 + (s - s')^2 + 3m_s^2(q^2 + s - s') + q^2(s + s')]\}, \quad (54)$$

$$-2m_b^2[m_d^2(q^4 - 2s^2 + q^2(s - 2s') + ss' + s'^2) + s((q^2 - s)^2 + (q^2 + s)q^2 - 2s'^2 + 3m_s^2(s + s' - q^2))].$$

The nonperturbative contributions to the correlators are calculated by taking the operators with dimensions $d = 3(\langle \bar{q}q \rangle)$ and $d = 5(m_0^2 \langle \bar{q}q \rangle)$ into account. For the $\langle K_{1A} | J_\mu | B \rangle$ matrix elements nonperturbative parts of the correlators are calculated as

$$\Pi_{AA} = (M + m) \langle \bar{q}q \rangle \left\{ \frac{1}{rr'} \right\} + m_0^2 (M + m) \langle \bar{q}q \rangle \left\{ \frac{1}{8rr'^2} - \frac{m_s^2}{2rr'^3} \right. \quad (55)$$

$$\left. - \frac{m_b^2}{2r^3r'} + \frac{1}{8r^2r'} + \frac{m_b^2 - q^2}{r^2r'^2} \right\},$$

$$\Pi_{V_{1A}} = \frac{\langle \bar{q}q \rangle}{M + m} \left\{ \frac{(m_b - m_s)^2 - q^2}{2rr'} \right\} \quad (56)$$

$$+ \frac{m_0^2 \langle \bar{q}q \rangle}{M + m} \left\{ \frac{(q^2 - (m_b - m_s)^2)m_s^2}{4rr'^3} + \frac{(q^2 - (m_b - m_s)^2)m_b^2}{4r^3r'} \right. \\ \left. + \frac{m_b^2 + 7m_b m_s - q^2}{8rr'^2} + \frac{m_s^2 + 7m_b m_s - q^2}{8r^2r} \right. \\ \left. + \frac{((m_b - m_s)^2 - q^2)(m_b^2 + m_s^2 - q^2)}{r^2r'^2} \right\},$$

$$\Pi_{V_{2A}} = (M + m) \langle \bar{q}q \rangle \left\{ \frac{1}{2rr'} \right\} \quad (57)$$

$$- m_0^2 (M + m) \langle \bar{q}q \rangle \left\{ \frac{m_s}{4rr'^3} - \frac{1}{16rr'^2} \right. \\ \left. + \frac{1}{16r'^2r^2} + \frac{m_b}{4r^3r'} \right. \\ \left. + \frac{q^2 - m_s^2 - m_b^2}{16r^2r'^2} \right\},$$

$$\Pi_{V_{3A}} = -(M + m) \langle \bar{q}q \rangle \left\{ \frac{1}{2rr'} \right\} \quad (58)$$

$$+ m_0^2 (M + m) \langle \bar{q}q \rangle \left\{ \frac{m_s}{4rr'^3} - \frac{1}{16rr'^2} + \frac{3}{16r'^2r^2} \right. \\ \left. + \frac{m_b}{4r^3r'} + \frac{q^2 - m_s^2 - m_b^2}{16r^2r'^2} \right\},$$

$$\Pi_{T_{1A}} = -\langle \bar{q}q \rangle \left\{ \frac{(m_b)}{16rr'} \right\} - m_0^2 \langle \bar{q}q \rangle \left\{ \frac{m_s^2(m_b - m_s)}{rr'^3} + \frac{m_b^2(m_b - m_s)}{r^3r'} \right. \quad (59)$$

$$\left. - \frac{(m_b + 8m_s)}{8rr'^2} + \frac{(m_b + m_s)}{8r^2r'} - \frac{(m_b - m_s)(m_b^2 - q^2)}{8r^2r'^2} \right\},$$

$$\Pi_{T_{2A}} = -\frac{\langle \bar{q}q \rangle}{M^2 - m^2} \left\{ \frac{(m_b)(8m_b^2 - 9m_s^2 + 8m_b(m_b - 2m_s) - 8q^2)}{rr'} \right\} \quad (60)$$

$$- \frac{m_0^2 \langle \bar{q}q \rangle}{M^2 - m^2} \left\{ \frac{m_b^2(m_b + m_s)(m_b^2 - 2m_b m_s - q^2)}{4r^3r'} \right. \\ \left. - \frac{[2m_b^3 + 7m_b^2 m_s - m_s(7m_b^2 - 2m_s^2 + 7q^2) + 2m_b(-m_s^2 - q^2)]}{16rr'^2} \right. \\ \left. + \frac{[9m_b^3 + 2m_s q^2 + m_b(-14m_s^2 + 7q^2)]}{16r^2r'} \right. \\ \left. - \frac{(m_b + m_s)(m_b^2 - q^2)(m_b^2 - 2m_b m_s - q^2)}{16r^2r'^2} \right. \\ \left. + \frac{m_s^2(m_b + m_s)(m_b^2 - 2m_b m_s - q^2)}{4rr'^3} \right\},$$

$$\Pi_{T_{3A}} = \langle \bar{q}q \rangle \left\{ \frac{m_b}{16rr'} \right\} + m_0^2 \langle \bar{q}q \rangle \left\{ \frac{m_s^2(m_b - m_s)}{4rr'^3} + \frac{m_b^2(m_b - m_s)}{4r^3r'} \right. \quad (61)$$

$$\left. + \frac{(8m_b + m_s)}{16r^2r'} - \frac{(m_b - m_s)(m_b^2 - q^2)}{16r^2r'^2} + \frac{(m_b + 8m_s)}{8rr'^2} \right\}.$$

For the $\langle K_{1B}|J_\mu|B\rangle$ matrix elements the nonperturbative parts of the correlators are calculated as

$$\Pi_{A_B} = 0, \quad (62)$$

$$\begin{aligned} \Pi_{V_{1B}} = & \frac{\langle\bar{q}q\rangle}{M+m}\left\{\frac{m_b}{rr'}\right\} - \frac{m_0^2\langle\bar{q}q\rangle}{M+m}\left\{\frac{m_s^2m_b}{2r'^3r} + \frac{m_sm_b^2}{2r^3r}\right. \\ & \left. + \frac{(m_b+m_s)}{8r'^2r} + \frac{7m_b}{8r'r^2} + \frac{m_b(q^2-m_b^2-m_s^2)}{8r^2r'^2}\right\}, \end{aligned} \quad (63)$$

$$\Pi_{V_{2B}} = 0, \quad (64)$$

$$\Pi_{V_{3B}} = 0, \quad (65)$$

$$\Pi_{T_{1B}} = 0, \quad (66)$$

$$\begin{aligned} \Pi_{T_{2B}} = & -\frac{\langle\bar{q}q\rangle}{M^2-m^2}\left\{\frac{m_s(m_b+m_s)}{rr'}\right\} + \frac{m_0^2\langle\bar{q}q\rangle}{M^2-m^2}\left\{\frac{m_s^3(m_b+m_s)}{2r'^3r} + \frac{m_b^3(m_b+m_s)}{2r^3r'}\right. \\ & \left. - \frac{m_s(m_b+m_s)(m_b^2-q^2)}{8r^2r'^2} + \frac{7m_bm_s}{8r'^2r} - \frac{m_b^2+m_s^2-7m_bm_s}{8r'r^2}\right\}, \end{aligned} \quad (67)$$

$$\Pi_{T_{3B}} = m_0^2\langle\bar{q}q\rangle\left\{\frac{1}{8r^2r'} - \frac{1}{8r'r^2}\right\}. \quad (68)$$

In the expressions of non-perturbative contributions to correlator (Eqs. 55 to 68), the first terms in brackets which are proportional to $\langle\bar{q}q\rangle$ are $d = 3$ dimensional, and the second terms in brackets which are proportional to $m_0^2\langle\bar{q}q\rangle$ are $d = 5$ dimensional contributions corresponding to operators $\langle\bar{q}q\rangle$ and $\langle\bar{q}\sigma Gq\rangle$. The non-perturbative contributions coming from $d = 4$ dimensional operators which are proportional to $m_d\langle\bar{q}q\rangle$ and $\langle g^2G^2\rangle$ are neglected.

To obtain the final expression for the sum rules of the form factors, the quark hadron duality assumption, which states that the phenomenological and perturbative spectral densities give the same result when integrated over an appropriate interval, is used. The quark hadron duality is expressed as[30]

$$\left[\int_{s_0}^{\infty}\int_{s'_0}^{\infty} + \int_{s_0}^{\infty}\int_0^{s'_0} + \int_0^{s_0}\int_{s'_0}^{\infty}\right] ds ds' \{\rho_{f_i}^h(s, s', q^2) - \rho_{f_i}(s, s', q^2)\} = 0, \quad (69)$$

where s_0 and s'_0 are the continuum thresholds in s and s' channels, and $\rho^h(s, s', q^2)$ is the spectral density of the continuum in the phenomenological part.

After calculating all spectral densities and nonperturbative contributions to correlators, by equating the coefficients of the selected structures from the phenomenological side (Eqs. 25 and 26) and the theoretical side (Eqs. 27 and 28), the QCD sum rules for the form factors parameterizing $\langle K_{1(A,B)}|J_\mu|B\rangle$ matrix elements are found as

$$\begin{aligned} f_{i,A}(q^2) = & \frac{m_b+m_d}{f_A m_A F_B M^2} e^{\frac{M^2}{M_1^2}} e^{\frac{m^2}{M_2^2}} \\ & \left\{\frac{-1}{4\pi}\int_0^{s_0} ds \int_0^{s'_0} ds' \Theta \rho_{f_{i,A}}(s, s', q^2) e^{\frac{-s}{M_1^2}} e^{\frac{-s'}{M_2^2}} + \hat{\Pi}_{f_{i,A}}^{nonpert}\right\}, \end{aligned} \quad (70)$$

and

$$\begin{aligned} f_{i,B}(q^2) = & -i \frac{m_b+m_d}{f_B(1\text{GeV}) F_B M^2} e^{\frac{M^2}{M_1^2}} e^{\frac{m^2}{M_2^2}} \\ & \left\{\frac{-1}{4\pi}\int_0^{s_0} ds \int_0^{s'_0} ds' \Theta \rho_{f_{i,B}}(s, s', q^2) e^{\frac{-s}{M_1^2}} e^{\frac{-s'}{M_2^2}} + \hat{\Pi}_{f_{i,B}}^{nonpert}\right\}. \end{aligned} \quad (71)$$

where $\Theta \equiv \Theta(1 - f(s, s')^2)$ is the unit step function determining the integration region and $f(s, s')$ is the function defined in Eq. 32. The expressions for the form factors of $B \rightarrow K_1(1270, 1400)\ell^+\ell^-$ transitions are obtained by using Eq. 17.

IV. NUMERICAL RESULTS AND DISCUSSIONS

In this section, the numerical results for the $B \rightarrow K_1\ell^+\ell^-$ transitions are presented. The expressions of form factors and the effective Hamiltonian depend on the parameters M_1^2 , M_2^2 , s_0 , s'_0 , on the masses and decay constants of the

TABLE III: The values of the input parameters for numerical analysis.

INPUT PARAMETERS			
$M_B = 5279 \text{ MeV}$ $\tau_B = (1.525 \pm 0.002) \times 10^{-12} \text{ s}$. $F_B = 0.14 \pm 0.01 \text{ GeV}$ [11]			
$m_s = 95 \pm 25 \text{ MeV}$	$m_b = (4.7 \pm 0.07) \text{ GeV}$	$m_d = (3 - 7) \text{ MeV}$ [11]	$\langle \bar{q}q \rangle \equiv \langle \bar{d}d \rangle = -(240 \pm 10 \text{ MeV})^3$ [31]
$m_{K_1}(1270) = 1.27 \text{ GeV}$ $m_{K_1}(1400) = 1.40 \text{ GeV}$		$f_A = (250 \pm 13) \text{ MeV}$ $f_B = (190 \pm 10) \text{ MeV}$	
$m_A = (1.31 \pm 0.06) \text{ GeV}$		$m_B = (1.34 \pm 0.08) \text{ MeV}$ [11, 23, 24]	
$ V_{tb} = 0.77^{+0.18}_{-0.24}$		$ V_{ts} = (40.6 \pm 2.7) \times 10^{-3}$ [35]	
$C_{10} = -4.669$	$C_9^{eff} = 4.344$	$C_7^{eff} = -0.313$ [29]	
$G_F = 1.17 \times 10^{-5} \text{ GeV}^{-2}$		$\alpha = 1/129$ [11]	
$M_1^2 = 16 \pm 2 \text{ GeV}^2$	$M_2^2 = 6 \pm 1 \text{ GeV}^2$	$s_0 = 34 \pm 4 \text{ GeV}^2$	$s'_0 = 4 \pm 1 \text{ GeV}^2$

K_1 and B states, on the values of V_{ij} , and on the values of the Wilson coefficients C_7^{eff} , C_9^{eff} and C_{10} . The values of the input parameters are presented in table III.

The explicit expressions of the form factors in Eqs. 70 and 71 contain four auxiliary parameters: Borel parameters M_1^2 and M_2^2 , as well as the continuum thresholds s_0 and s'_0 . These are not physical quantities, hence the physical quantities, form factors, must be independent of these auxiliary parameters. The working region of M_1^2 and M_2^2 is determined by requiring that the higher state and continuum contributions are suppressed and the contribution of the highest order operator must be small. These conditions are both satisfied in the following regions; $12 \text{ GeV}^2 \leq M_1^2 \leq 20 \text{ GeV}^2$ and $4 \text{ GeV}^2 \leq M_2^2 \leq 8 \text{ GeV}^2$. The dependence of form factors T_{1A} and T_{1B} on Borel masses at $q^2 = 0$ are plotted in figures 2(a) and 2(b). From the figures it is found that the results are stable in the working region of Borel mass parameters.

The continuum thresholds s_0 and s'_0 are determined by two-point QCD sum rules and related to the energy of the excited states. The form factors which are the physical quantities defining the transitions, should be stable with respect to the small variations of these parameters. In general, the continuum thresholds are taken to be around $(m_{hadron} + 0.5)^2$ [32–34]. The dependence of form factors T_{1A} and T_{1B} on continuum thresholds at $q^2 = 0$ are plotted in figures 2(c) and 2(d). From the figures it is found that the results are stable for variations of s_0 and s'_0 .

The sum rules expressions for the form factors are truncated at 7 GeV^2 . In order to extend our results to the whole physical region, i.e., $0 \leq q^2 < (m_B - m_{K_1})^2$ and for the reliability of the sum rules in the full physical region, a fit parametrization is applied such that in the region $-10 \text{ GeV}^2 \leq q^2 \leq -2 \text{ GeV}^2$, where the spectral integrals can be handled safely by applying Cutkovsky rules. This parametrization coincides with the sum rules predictions. To find the extrapolation of the form factors in the whole physical region, the fit function is chosen as

$$f_i(q^2) = \frac{f_i(0)}{1 - a\hat{q} + b\hat{q}^2}. \quad (72)$$

The values for a , b and $f_i(0)$ are given in Table IV and V for the form factors of $\langle K_{1A} | J_\mu | B \rangle$ and $\langle K_{1B} | J_\mu | B \rangle$ matrix elements respectively. The errors in the values of $f_i(0)$ in tables IV and V are due to uncertainties in sum rule calculations and also due to errors in input parameters.

The q^2 dependence of $f_{i,A}$ and $f_{i,B}$, the sum rules predictions and also the fit results, are plotted in the range $-10 \leq q^2 \leq M^2 - m^2$ in figures 3 and 4. It is seen from tables IV and V, and from figures 3 and 4 that the form factors of $B \rightarrow K_{1A} \ell^+ \ell^-$ transition, i.e. $f_{i,A}$, and the form factors of $B \rightarrow K_{1B} \ell^+ \ell^-$ transition, i.e. $f_{i,B}$ are opposite in sign.

For the transitions to physical states, i.e. for $B \rightarrow K_1(1270, 1400) \ell^+ \ell^-$ transitions, the dependence of the form factors of $B \rightarrow K_1(1270) \ell^+ \ell^-$ on the mixing angle θ_{K_1} are plotted in figure 5, and the dependence of form factors of $B \rightarrow K_1(1400) \ell^+ \ell^-$ on the mixing angle θ_{K_1} are plotted in figure 6 at $q^2 = 0$. The region between two black dashed vertical lines is the region estimated as $\theta_{K_1} = (-34 \pm 13)^\circ$ [16]. It is seen from figures 5(a) and 5(b) that the absolute values the form factors of $B \rightarrow K_1(1270) \ell^+ \ell^-$ transition are maximum at $\theta_{K_1} = -(45 \pm 5)^\circ$, and their values are zero

TABLE IV: The fit parameters and coupling constants for $\langle K_{1A}|J_\mu|B\rangle$ matrix elements.

f_i	$f_i(0)$	a	b
A_A	0.47 ± 0.08	0.74	-0.41
V_{1A}	0.35 ± 0.07	0.52	-1.2
V_{2A}	0.36 ± 0.07	0.41	-0.74
V_{3A}	$-(0.39 \pm 0.08)$	0.45	-0.27
T_{1A}	0.38 ± 0.08	0.73	-0.36
T_{2A}	0.38 ± 0.09	0.67	-0.26
T_{3A}	0.36 ± 0.07	0.42	-0.15

TABLE V: The fit parameters and coupling constants for $\langle K_{1B}|J_\mu|B\rangle$ matrix elements.

f_i	$f_i(0)$	a	b
A_B	-0.31 ± 0.06	1.3	0.37
V_{1B}	-0.40 ± 0.08	1.4	-0.10
V_{2B}	-0.34 ± 0.06	1.2	0.37
V_{3B}	0.39 ± 0.08	1.1	0.46
T_{1B}	-0.22 ± 0.05	1.1	0.24
T_{2B}	-0.21 ± 0.07	1.3	0.081
T_{3B}	-0.26 ± 0.04	1.1	0.27

at $\theta_{K_1} = 42 \pm 5^\circ$. For the form factors of $B \rightarrow K_1(1400)\ell^+\ell^-$ transitions, it is seen from figures 6(a) and 6(b) that the absolute values of the form factors are maximum at $\theta_{K_1} = 40 \pm 5^\circ$, their values are zero at $\theta_{K_1} = -(47 \pm 7)^\circ$. Since the region $\theta_{K_1} = -(47 \pm 7)^\circ$ in which form factors are zero coincides with the region $\theta_{K_1} = (-34 \pm 13)^\circ$, to obtain a precise prediction of the form factors, the mixing angle should be determined more precisely.

Finally, the branching fractions to leptonic final states e^+e^- , $\mu^+\mu^-$ and $\tau^+\tau^-$ for $\theta_{K_1} = -34^\circ$ are also estimated by integrating the partial width in Eq. 10. The results are presented in table VI in comparison with the results found in [16]. The first errors in our results are due to uncertainties from sum rule calculations and input parameters, and the second errors are due to uncertainty in the mixing angle θ_{K_1} . Our results are in good agreement with the results found in [16].

TABLE VI: The branching fractions of $B \rightarrow K_1(1270, 1400)\ell^+\ell^-$ decays for $\theta_{K_1} = -34^\circ$.

mode	this work	[16]
$\mathcal{B}(K_1(1270)e^+e^-)$	$(2.11 \pm 0.82^{+0.42}_{-0.52}) \times 10^{-6}$	$(2.5^{+1.4+0.0}_{-1.1-0.3}) \times 10^{-6}$
$\mathcal{B}(K_1(1270)\mu^+\mu^-)$	$(2.10 \pm 0.81^{+0.41}_{-0.49}) \times 10^{-6}$	$(2.1^{+1.2+0.0}_{-0.9-0.2}) \times 10^{-6}$
$\mathcal{B}(K_1(1270)\tau^+\tau^-)$	$(0.42 \pm 0.21^{+0.11}_{-0.15}) \times 10^{-7}$	$(0.8^{+0.4+0.0}_{-0.3-0.1}) \times 10^{-7}$
$\mathcal{B}(K_1(1400)e^+e^-)$	$(1.1 \pm 0.4^{+0.4}_{-0.5}) \times 10^{-7}$	$(0.9^{+0.3+2.3}_{-0.3-0.4}) \times 10^{-7}$
$\mathcal{B}(K_1(1400)\mu^+\mu^-)$	$(1.0 \pm 0.4^{+0.4}_{-0.5}) \times 10^{-7}$	$(0.6^{+0.2+1.8}_{-0.1-0.2}) \times 10^{-7}$
$\mathcal{B}(K_1(1400)\tau^+\tau^-)$	$(0.3 \pm 0.2^{+0.1}_{-0.1}) \times 10^{-8}$	$(0.1^{+0.0+0.5}_{-0.0-0.1}) \times 10^{-8}$

The experimental bounds on $B \rightarrow K_1(1270, 1400)\ell^+\ell^-$ decays can be obtained from the inclusive $B \rightarrow X_s\ell^+\ell^-$ decays. The current averages on inclusive decays are[35, 36]:

$$\begin{aligned}\mathcal{B}(B \rightarrow X_s e^+ e^-) &= (4.7 \pm 1.3) \times 10^{-6} [(4.91_{-1.06}^{+1.04}) \times 10^{-6}], \\ \mathcal{B}(B \rightarrow X_s \mu^+ \mu^-) &= (4.3 \pm 1.2) \times 10^{-6} [(2.23_{-0.98}^{+0.97}) \times 10^{-6}], \\ \mathcal{B}(B \rightarrow X_s \ell^+ \ell^-) &= (4.5 \pm 1.0) \times 10^{-6} [(3.66_{-0.77}^{+0.76}) \times 10^{-6}],\end{aligned}\tag{73}$$

where the first averages are from PDG[35], and the second values in square brackets are the recent HFAG averages[36].

The results found in this work (table VI) are consistent with these average values except $B \rightarrow K_1(1270)\mu^+\mu^-$. For $b \rightarrow s\mu^+\mu^-$ channel, when the measured branching fractions of exclusive decays $B \rightarrow K\mu^+\mu^-$ and $B \rightarrow K^*\mu^+\mu^-$ which amount $(1.63 \pm 0.21) \times 10^{-6}$ [35] are considered, the room left for other exclusive decays including $B \rightarrow K_1(1270)\mu^+\mu^-$ is about $(0.6 \sim 2.6) \times 10^{-6}$. However when the errors are considered, even this channel is still consistent with the data. And also when the dependence of branching ratios on θ_{K_1} are considered (fig. 7), it can be seen that the value of the branching ratio of the $B \rightarrow K_1(1270)\mu^+\mu^-$ can be smaller depending on the mixing angle θ_{K_1} .

In conclusion, we have calculated the form factors of $B \rightarrow K_{1(A,B)}\ell^+\ell^-$ transitions using three point QCD sum rules approach. We analyzed the q^2 behaviors of the form factors of $B \rightarrow K_{1(A,B)}\ell^+\ell^-$ transitions. Considering the axial vector mixing angle θ_{K_1} , we estimated the form factors of $B \rightarrow K_1(1270, 1400)\ell^+\ell^-$ transitions, i.e. transitions into physical states and analyzed their dependence on the mixing angle θ_{K_1} at $q^2 = 0$. Using these results we estimated the branching fractions into final leptonic states. We conclude that the transitions $B \rightarrow K_1(1270, 1400)\ell^+\ell^-$ can be observed at LHC and further B factories and measurements on the mixing angle θ_{K_1} can be performed.

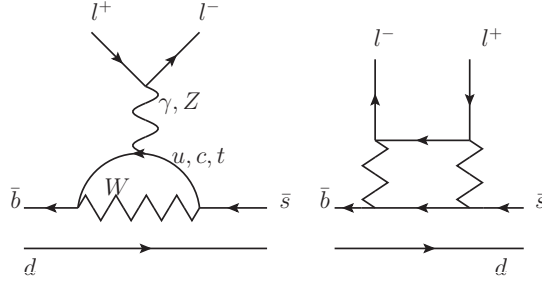
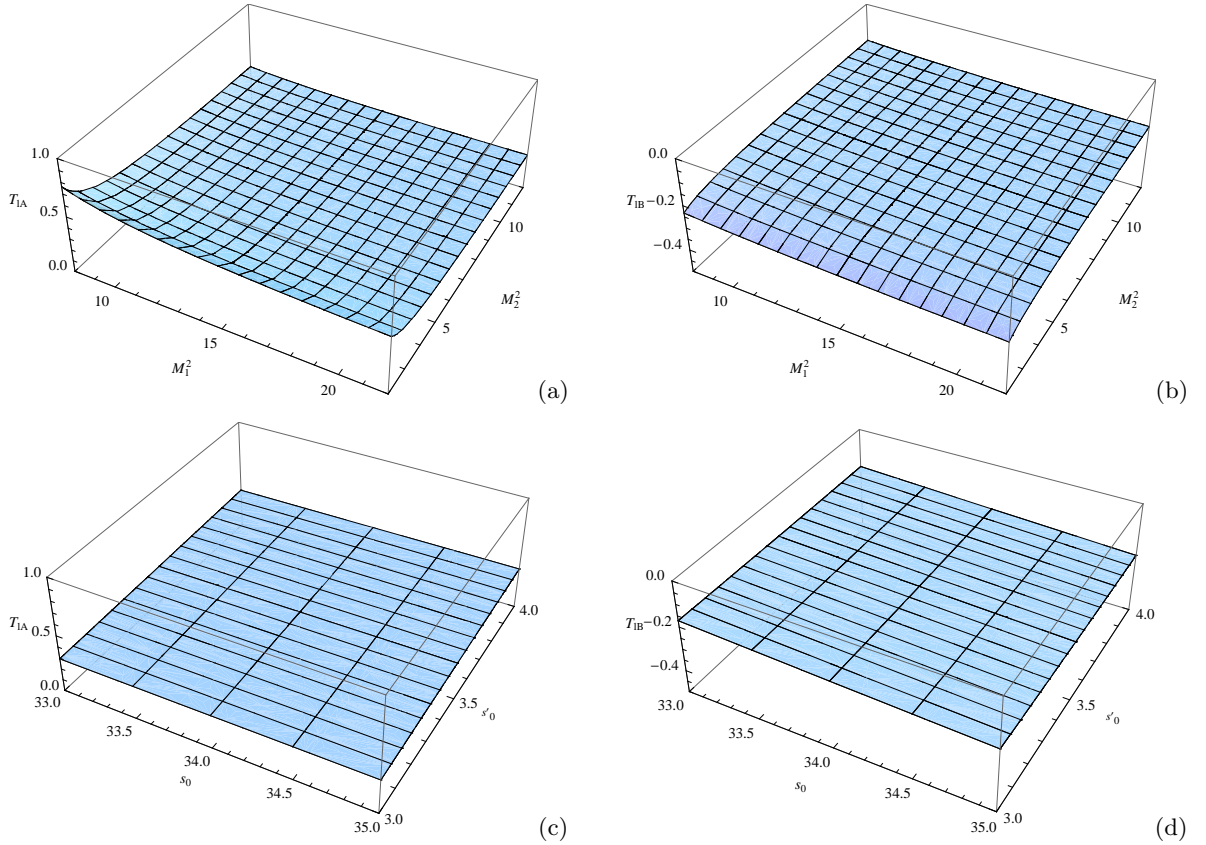
Acknowledgments

The authors would like to thank to T. M. Aliev, H. D. thanks to G. Erkol, J. Smith and K. Azizi, A.Ö. thanks to K.-C. Yang for useful discussions during this work. The work of A.Ö. have been been supported in part by the European Union (HadronPhysics2 project Study of strongly interacting matter.).

-
- [1] B. Aubert *et al.* [BABAR Collaboration], Phys. Rev. D **70**, 112006 (2004) [arXiv:hep-ex/0407003].
 - [2] M. Nakao *et al.* [Belle Collaboration], Phys. Rev. D **69**, 112001 (2004) [arXiv:hep-ex/0402042].
 - [3] T. E. Coan *et al.* [CLEO Collaboration], Phys. Rev. Lett. **84**, 5283 (2000) [arXiv:hep-ex/9912057].
 - [4] H. Yang *et al.*, Phys. Rev. Lett. **94**, 111802 (2005) [arXiv:hep-ex/0412039].
 - [5] A. Ishikawa *et al.* [Belle Collaboration], Phys. Rev. Lett. **91**, 261601 (2003) [arXiv:hep-ex/0308044].
 - [6] B. Aubert *et al.* [BABAR Collaboration], Phys. Rev. D **73**, 092001 (2006) [arXiv:hep-ex/0604007].
 - [7] A. Ishikawa *et al.* [Belle Collaboration], Phys. Rev. Lett. **96**, 251801 (2006) [arXiv:hep-ex/0603018].
 - [8] B. Aubert *et al.* [BABAR Collaboration], arXiv:0804.4412 [hep-ex].
 - [9] B. Aubert *et al.* [BABAR Collaboration], arXiv:0807.4119 [hep-ex].
 - [10] K. Abe *et al.*, [BELLE Collaboration], BELLE-CONF-0411, arXiv:0408138[hep-ex].
 - [11] C. Amsler *et al.*, Particle Data Group, Phys. Lett. B 667 1 (2008).
 - [12] A Augusto Alves Jr *et al.*, The LHCb Collaboration, JINST **3** S08005(2008).
 - [13] SuperB Collaboration, *SuperB: A High-Luminosity Asymmetric e^+e^- Super Flavor Factory. Conceptual Design Report*, INFN/AE - 07/2, SLAC-R-856, LAL 07-15, arXiv:0709.0451v2[hep-ex].
 - [14] M-O Bettler *et al.*, for the LHCb collaboration, CERN-LHCB-CONF-2009-038, LPHE-2009-05, arXiv:0910.0942[hep-ex].
 - [15] K.-C. Yang, Phys.Rev.**D78** (2008) 034018, arXiv:0807.1171v3 [hep-ph].
 - [16] H. Hatanaka, K.-C. Yang, Phys. Rev. **D 77** (2008) 094023.
 - [17] S. R. Choudhury, A. S. Cornell, N. Gaur, Eur.Phys.J.**C58**(2008)251-259, arXiv:0707.0446[hep-ph].
 - [18] V. Bashiry, JHEP 0906(2009)062, arXiv:0902.2578[hep-ph].
 - [19] V. Bashiry, K. Azizi, arXiv:0903.1505[hep-ph]
 - [20] M. A. Paracha, I. Ahmed and M. J. Aslam, Eur. Phys. J. C **52**, 967 (2007), arXiv:0707.0733 [hep-ph].
 - [21] I. Ahmed, M. A. Paracha and M. J. Aslam, Eur. Phys. J. C **54**, 591 (2008), arXiv:0802.0740 [hep-ph].
 - [22] A. Saddique, M. J. Aslam and C. D. Lu, arXiv:0803.0192 [hep-ph].
 - [23] J. P. Lee, Phys. Rev. **D 74** (2006) 074001.
 - [24] K.-C. Yang, Nucl.Phys.B776(2007)187-257.
 - [25] H. Y. Cheng, C. K. Chua, Phys. Rev. **D 69** (2004) 094007.
 - [26] C. Garcia-Recio, L.S. Geng, J. Nieves and L.L. Salcedo, arXiv:1005.0956[hep-ph].

- [27] M. Suzuki, arXiv:9703271[hep-ph] Phys. Rev. D **47**, 1252 (1993).
- [28] L. Burakovsky and T. Goldman, Phys. Rev. D **57**, 2879 (1998), .
- [29] A. J. Buras, M. Munz, Phys. Rev. **D 52** (1995) 186.
- [30] P. Colangelo, F. De Fazio, P. Santorelli and E. Scrimieri, Phys.Rev. **D53** (1996) 3672-3686.
- [31] B.L. Ioffe, Prog. Part. Nucl. Phys. **56**, 232(2006).
- [32] T. M. Aliev, M. Savci, Phys. Lett. **B 434** (1998) 358.
- [33] M. A. Shifman, A. I. Vainshtein, V. I. Zakharov, Nucl. Phys. **B147** (1979) 385.
- [34] P. Colangelo, F. De Fazio, A. Ozpineci, Phys. Rev. **D72**, (2005) 074004.
- [35] K. Nakamura et al. (Particle Data Group), J. Phys. G 37, 075021 (2010).
- [36] E. Barberio *et al*, HFAG(Heavy Flavor Averaging Group), arXiv:0809.1297v3[hep-ex],online update at <http://www.slac.stanford.edu/xorg/hfag>.

Appendix A: Figures

FIG. 1: The loop penguin and box diagrams contributing to semileptonic B to K_1 transitions.FIG. 2: (a,b):The dependence of the form factors T_{1A} (a) and T_{1B} (b) on Borel mass parameters M_1^2 and M_2^2 at $q^2 = 0$ for $s_0 = 34\text{GeV}^2$ and $s'_0 = 4\text{GeV}^2$.(c,d): The dependence of the form factors T_{1A} (c) and T_{1B} (d) on continuum thresholds s_0 and s'_0 at $q^2 = 0$ for $M_1^2 = 16\text{GeV}^2$ and $M_2^2 = 6\text{GeV}^2$.

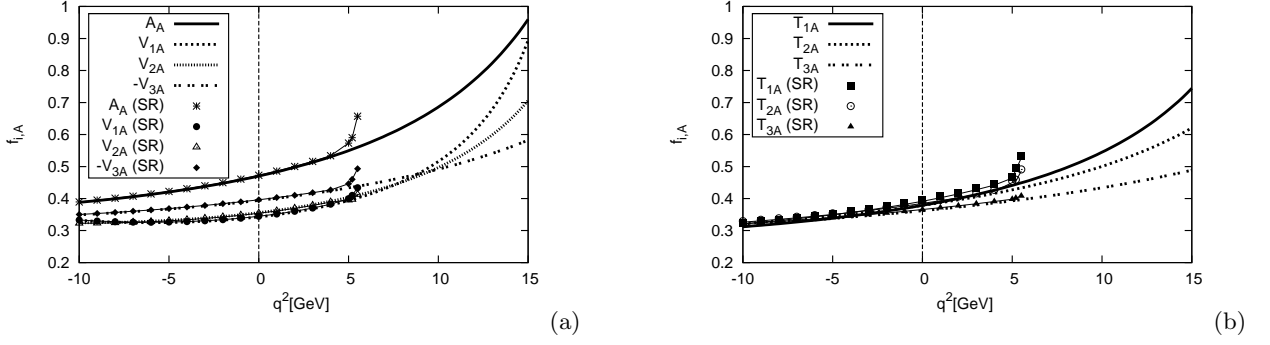


FIG. 3: The q^2 dependence of the vector form factors(a) and tensor form factors(b) of $\langle K_{1A} | J_\mu | B \rangle$ matrix element. The sum rules predictions for the form factors also shown with data points connected with a thin line.

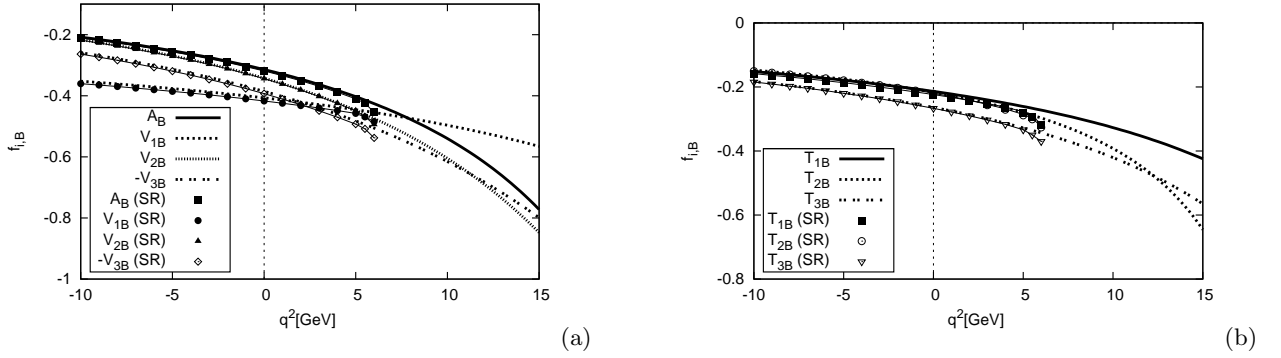


FIG. 4: The q^2 dependence of the vector form factors(a) and tensor form factors(b) of $\langle K_{1B} | J_\mu | B \rangle$ matrix element. The sum rules predictions for the form factors also shown with π data points connected with a thin line.

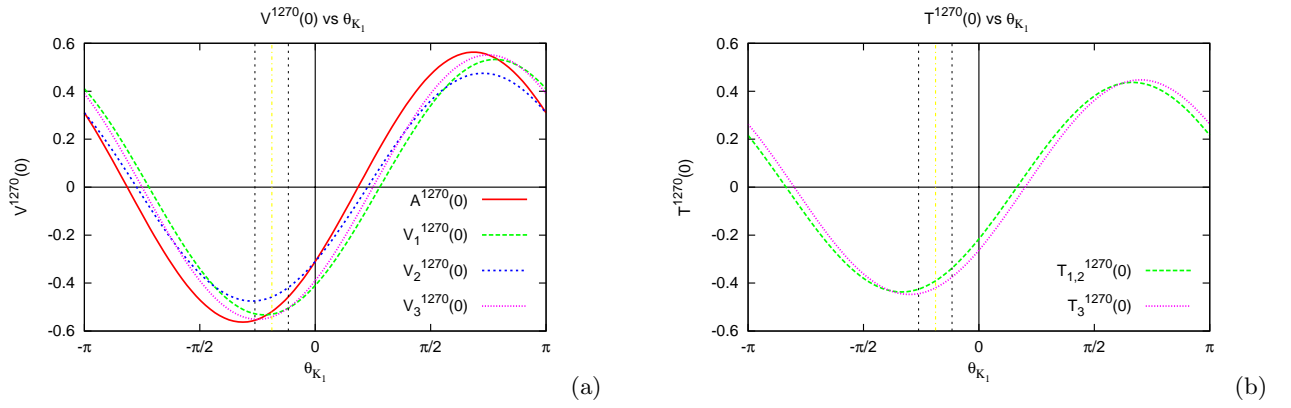


FIG. 5: The θ_{K_1} dependence of the vector form factors(a) and tensor form factors(b) of $B \rightarrow K_1(1270) \ell^+ \ell^-$ at $q^2 = 0$.

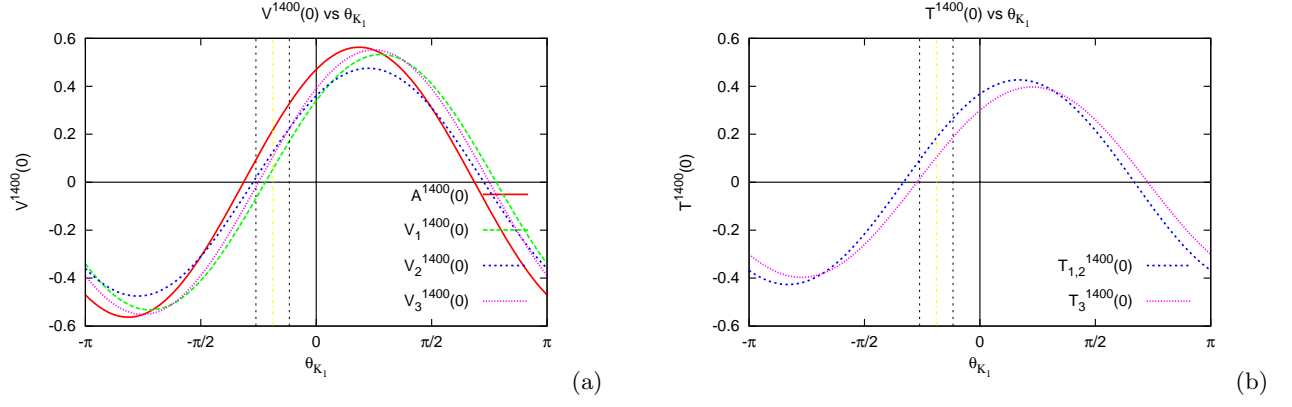


FIG. 6: The θ_{K_1} dependence of the vector form factors(a) and tensor form factors(b) of $B \rightarrow K_1(1270)\ell^+\ell^-$ at $q^2 = 0$.

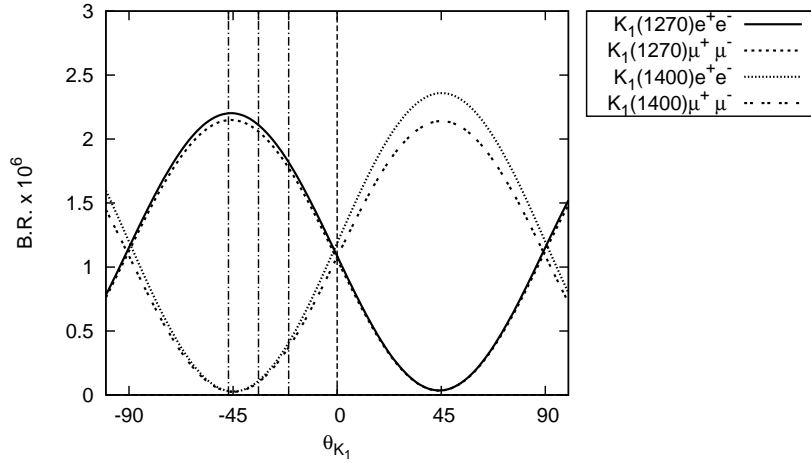


FIG. 7: The θ_{K_1} dependence of the branching ratios of $B \rightarrow K_1(1270)e^+e^-$ (solid), $B \rightarrow K_1(1270)\mu^+\mu^-$ (dashed), $B \rightarrow K_1(1400)e^+e^-$ (dotted) and $B \rightarrow K_1(1400)\mu^+\mu^-$ (double dashed) channels.